Pillared Two-Dimensional Metal−Organic Frameworks Based on a Lower-Rim Acid Appended Calix[4]arene
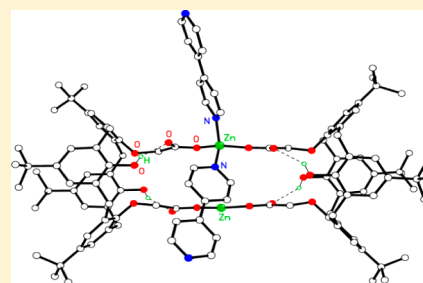
Carl Redshaw,*,[†] Oliver Rowe,[‡] Mark R. J. Elsegood,[§] Lynne Horsburgh,[§] and Simon J. Teat[#]

[†]Department of Chemistry, University of Hull, Hull HU6 7RX, U.K.

[‡]Energy Materials Laboratory, School of Chemistry, University of East Anglia, Norwich, NR4 7TJ, U.K.

[§]Chemistry Department, Loughborough University, Loughborough, Leicestershire, LE11 3TU, U.K.

[#]Advanced Light Source, Berkeley National Lab, 1 Cyclotron Road, Berkeley, California 94720, United States

S *Supporting Information*

ABSTRACT: Solvothermal reactions of the lower-rim functionalized diacid calix[4]arene 25,27-bis(methoxycarboxylic, acid)-26,28-dihydroxy-4-*tert*-butylcalix[4]arene, (LH_2) with $Zn(NO_3)_2 \cdot 6H_2O$ and the dipyridyl ligands 4,4′-bipyridyl (4,4′-bipy), 12-di(4-pyridyl)ethylene (DPE), or 4,4′-azopyridyl (4,4′-azopy) afforded a series of two-dimensional structures of the formulas $\{[Zn(4,4′\text{-bipy})(\mathbf{L})] \cdot 2^{1}/_{4}DEF\}_n$, (**1**), $\{[Zn_2(\mathbf{L})(DPE)] \cdot DEF\}_n$ (**2**), and $\{[Zn(OH_2)_2(\mathbf{L})(4,4′\text{-azopy})] \cdot DEF\}_n$ (**3**) (DEF = diethylformamide).

INTRODUCTION

The calixarene family has attracted attention over the past decade for a multitude of applications,[1] including gas uptake in the solid state.[2] Given the interest in metal−organic frameworks (MOFs), the incorporation of such cavity-containing species offers great potential. The reaction of upper-rim functionalized calix[4]arenes (or thiacalixarenes or sulfonylcalixarenes) with the late transition metals (or lanthanides) gives a variety of two- and three-dimensional (2-D and 3-D) frameworks, with the dimensionality of the resulting materials dictated by the nature of the secondary building unit (SBU).[3,4] However, with the exception of the example reported by Liu et al.,[4] the use of lower-rim acid-functionalized analogues leads to the synthesis of only one-dimensional (1-D) coordination polymers, exhibiting nanotube and chain morphologies, with thermogravimetric analysis (TGA) and gas uptake analyses of these structures demonstrating a lack of porosity. To synthesize porous frameworks using the lower-rim functionalized calix[4]-arene linker, some means of increasing the dimensionality of these structures is required, and it is with this in mind that our attention was drawn to the chain structures $[Li_4(\mathbf{L})_2(EtOH)_2]$ and $[Zn(\mathbf{L})_2(DMF)(H_2O)]_n$ (**L** = 25,27-bis(methoxycarboxylic acid)-26,28-dihydroxycalix[4]arene, DMF = *N,N*-dimethylformamide).[5] In both of these examples, the presence of coordinated solvent molecules is reminiscent of the $[Zn(BDC)\cdot(DMF)(H_2O)]_n$ (BDC = benzene-1,4-dicarboxylate) structure and many others, in which the substitution of apically coordinated water molecules with neutral pillaring linkers gives rise to a multitude of porous 3-D structures. We therefore embarked on a program of research involving the reaction of the potential anionic linker LH_2 with zinc nitrate and the neutral pillaring linkers 4,4′-bipyridyl (4,4′-bipy), 1,2-di(4-pyridyl)ethylene (DPE), and 4,4′-azopyridyl (4,4′-azopy) with a view to the synthesis of multidimensional porous MOFs. It was hoped that the inclusion of the bipyridyl linkers would give rise to 3-D structures exhibiting novel network topologies and hierarchical porosity. While no literature examples exist of the use of neutral pillaring linkers with acid functionalized calix[4]arenes in MOF synthesis, early research conducted by Atwood and MacGillivray reveals the potential for increased dimensionality in hydrogen-bound multicomponent systems involving the related molecule *C*-methylcalix[4]resorcinarene.[6] The successful synthesis of crystalline *C*-methylcalix[4]-resorcinarene(pyridine)$_4$·2pyridine, a monomeric species in which four pyridine molecules are hydrogen bonded to the hydroxyl functions of the calix[4]resorcinarene via the pyridinyl nitrogens, was followed by the substitution of the pyridine with 4,4′-bipy. The resulting crystalline product, bearing the formula *C*-methylcalix[4]resorcinarene(4,4′-bipy)$_2$ exhibits 1-D chains formed by the H-bonding of two 4,4′-bipy units per *C*-methylcalix[4]resorcinarene unit in a bridging fashion.

Subsequent work by Coppens and co-workers using hydrothermal conditions to explore the H-bonding behavior of *C*-methylcalix[4]resorcinarene and the bipyridyls 4,4′-bipy and DPE reveals the synthesis of 2- and 3-D H-bonded structures,[7] with further examples of multidimensional H-bonded networks of this type incorporating longer bipyridyls reported by Nakamura et al.[8] In all of these examples, the cavities formed by the interaction of the component molecules are capable of hosting guest molecules, and in many cases, the
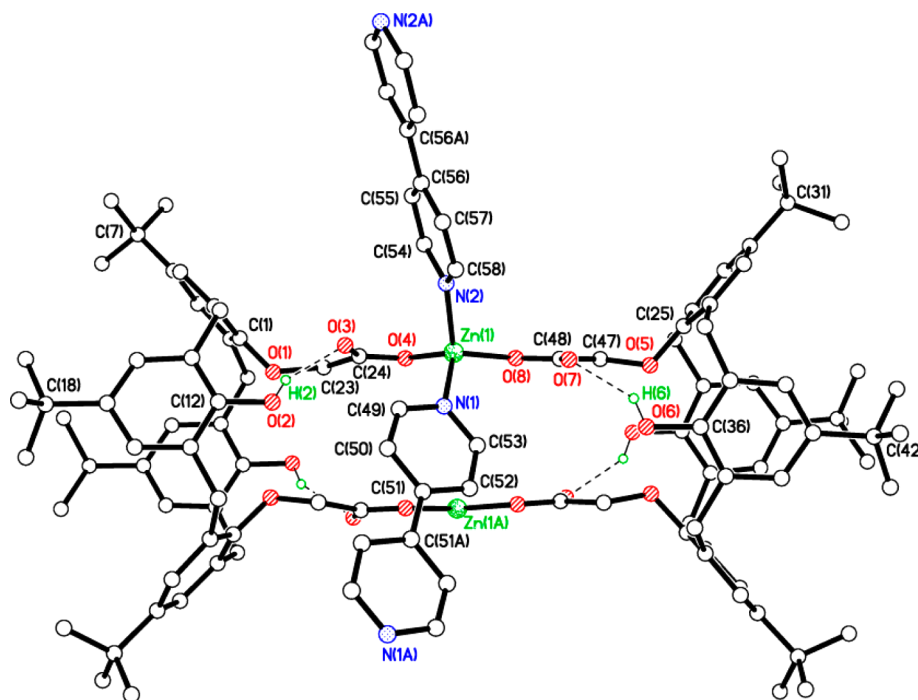
Figure 1. Diagram of the $Zn_2(L)_2(4,4'\text{-bipy})_2$ dimer in **1**, showing the coordination environment around the metal centers. Hydrogen atoms, except those involved in H-bonding interactions, are omitted. Hydrogen bonds are represented by dotted lines. Selected bond lengths (Å) and angles (°): Zn(1)−N(1) 1.987(4), Zn(1)−N(2) 1.970(5), Zn(1)−O(4) 1.951(3), Zn(1)−O(8) 1.893(3); N(1)−Zn(1)−N(2) 106.96(19), O(4)−Zn(1)−O(8) 101.29(12), C(1)−O(1)−C(23) 116.0(3), C(25)−O(5)−C(47) 116.1(3).

topology of the H-bonded networks is determined by the size and shape of the guest. It is therefore reasonable to assume that the employment of these principles in the calixarene coordination chemistry environment will also afford multi-dimensional structures capable of incorporating guest molecules.

■ RESULTS AND DISCUSSION

The solvothermal reaction of LH_2 with 4,4′-bipy and zinc nitrate in a diethylformamide (DEF)/methanol mixture afforded **1** as colorless prisms in good yield. The crystals were of suitable quality for single crystal X-ray diffraction, although requiring the use of synchrotron radiation to provide an adequate data set.[9] Elucidation of the structure reveals the self-assembly of a 2-D extended bilayer structure of the formula $\{[Zn(4,4'\text{-bipy})(L)]\cdot2\frac{1}{4}DEF\}_n$ formed by the coordination of 4,4′-bipy molecules to Zn_2L_2 dimers. Each of the dimers comprises two calix[4]arene molecules linked through two zinc atoms via the coordination of their carboxylate groups. These carboxylate groups adopt a monodentate binding mode, the unbound carboxylate oxygen involved in H-bonding to the phenolic −OH groups of the parent calixarene, with two 4,4′-bipy molecules per metal giving a tetrahedral coordination geometry (Figure 1).

The 4,4′-bipy molecules extend in four divergent directions in the *ac* plane, linking the dimers to their four nearest neighbors to give the extended 2-D structure with sheets observed in the *ac* plane (Figures 2 and S1, Supporting Information). Two large cavities per unit cell, located around the neutral linkers, contain highly disordered solvent molecules which were modeled as areas of diffuse electron density using the PLATON squeeze procedure,[10] giving approximately 9 DEF molecules per void, or 18 per unit cell.
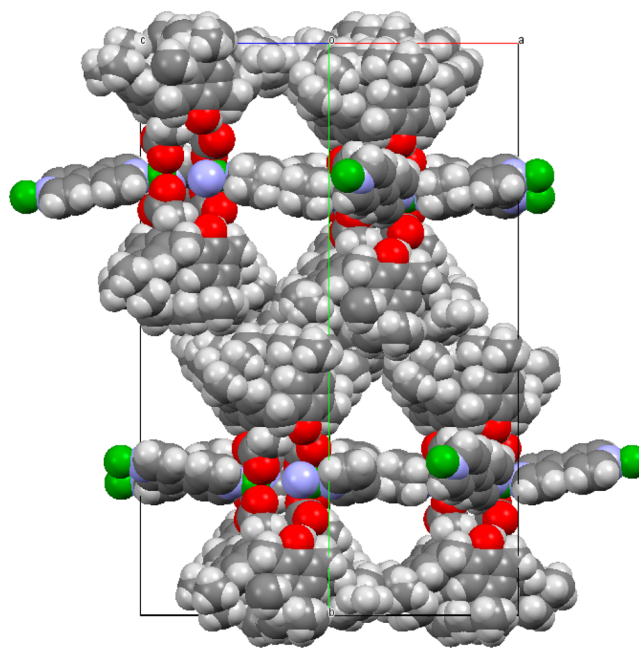

Figure 2. Packing plot of **1** using space filling atoms.

No guest solvent molecules are observed inside the calix[4]arene bowl, due to the pinched cone conformation adopted by the molecule (Figure 3). This conformation may result from the intramolecular H-bonding observed between the H(2)/H(6) hydrogens and the O(3)/O(7) oxygens which reduces the angle between the nonfunctionalized phenol units, or by the conformation adopted by the acid moieties, which forces the acid appended phenol units to swing outward. The pinched cone conformation can be quantified by comparing the
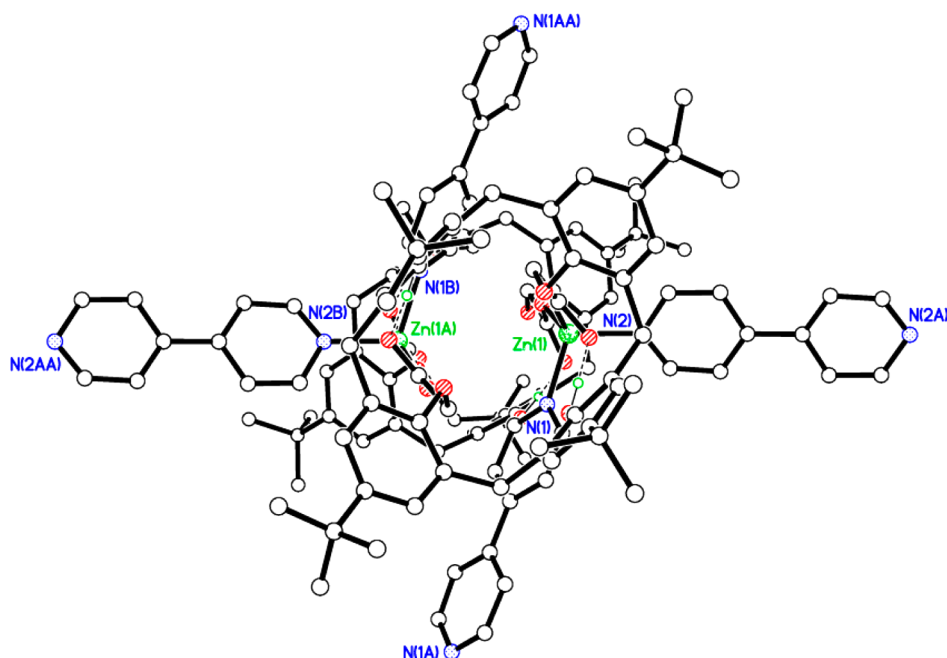
Figure 3. Diagram of **1** viewed through the annulus of the calix[4]arene molecule showing the pinched conformation adopted in this structure. Carbon atoms are represented by empty circles, with nitrogen, oxygen, and zinc atoms colored blue, red, and green respectively. Hydrogen atoms, except those involved in H-bonding, which are represented by small green circles, are omitted.

angles subtended by the calixarene phenolic C_6 rings and the basal plane defined by the four phenolic oxygen atoms: 42.87(9)° for C(1) > C(6), 40.74(8)° for C(25) > C(30), 86.33(10)° for C(12) > C(17), and 88.36(9)° for C(36) > C(41)°.

The solvothermal reaction of LH_2 with DPE and zinc nitrate in a DEF/methanol mixture afforded **2** as pale yellow prisms in moderate yield. The crystals were of sufficient quality for elucidation by single crystal X-ray diffraction, revealing a 2-D structure of the formula $\{[Zn_2(\mathbf{L})_2(DPE)]\cdot DEF\}_n$. The structure of **2** differs from that of **1** in both carboxylate coordination mode and packing. In this example, four neighboring calix[4]arene units are linked via the coordination of one of the appended acid moieties in a di-monodentate fashion, bridging two zinc centers, giving the paddlewheel SBU (Figure 4). This coordination mode is observed at each of the acid moieties, giving infinite chains of the formula Zn**L**, observed along the *a* axis.

Coordination of the neutral pillaring linker to these paddlewheel SBUs above and below the plane of the carboxylate functions gives a distorted square-based pyramidal coordination geometry around the metal centers, and further links the Zn**L** chains into the extended 2-D bilayer structure observed in the *ab* plane (Figures 5 and S2). The pyridinyl ligands in this example are disordered over two positions, with only the position of the coordinating N atom common to both components. Likewise, all four tertiary butyl groups per calix[4]arene unit were disordered and modeled over two positions. Guest solvent atoms could not be resolved by point atom observations due to disorder; hence, the PLATON squeeze procedure was performed.[10] This recovered 89 electrons situated in one large void and six much smaller voids per unit cell. As the smaller voids are not large enough to accommodate DEF or MeOH guest molecules, their electron contribution was omitted, giving a total of one guest DEF per large void or one per formula unit. It is of note that due to the
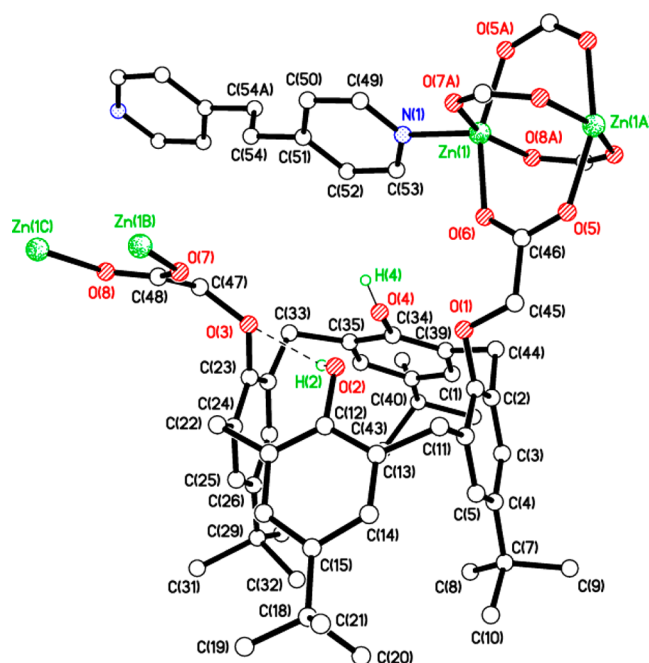

Figure 4. Diagram of the coordination environment around the metal centers in **2**. Hydrogen atoms, except those involved in H-bonding have been omitted. Selected bond lengths (Å) and angles (°): Zn(1)−N(1) 2.022(6), Zn(1)−O(5A) 2.052(4), Zn(1)−O(6) 2.053(5), Zn(1)−O(7A) 2.055(5), Zn(1)−O(8A) 2.057(5); N(1)−Zn(1)−O(8A) 102.1(2), O(1)−C(45)−C(46) 112.5(6).

disordered nature of the DPE linker, the dimensions of the large void are subject to variation, and hence some may accommodate more than one DEF molecule.

As with the previous structure, the calix[4]arene adopts a pinched conformation precluding the presence of solvent molecules within the bowl; however, in this example it is the acid-appended phenol units which are forced to swing inward
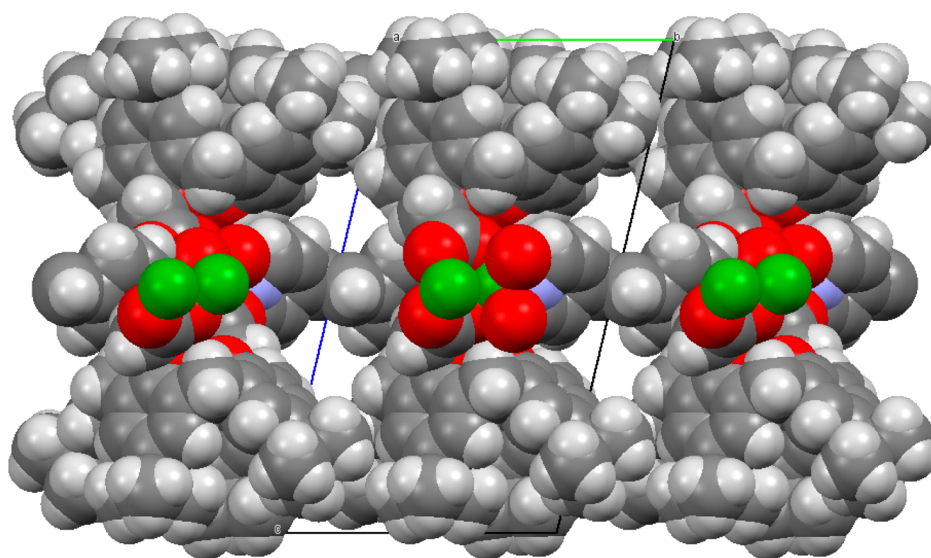
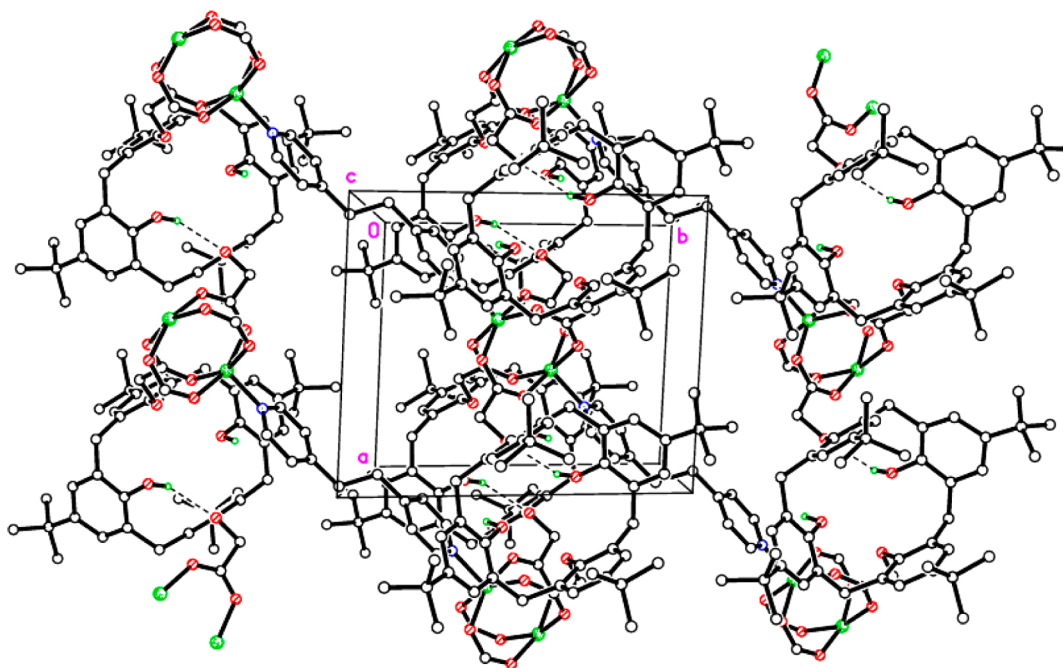**Figure 5.** Packing plot of **2** using space filling atoms.

Figure 6. Diagram of **2** as viewed along the *c* axis showing the pinched bowl conformation adopted by the calix[4]arene molecule. Carbon atoms are represented by empty circles, with nitrogen, oxygen, and zinc atoms colored blue, red, and green respectively. Hydrogen atoms, except those involved in H-bonding, which are represented by small green circles, are omitted.

to allow the acid moiety to participate in binding to the paddlewheel SBU (Figure 6). Angles subtended by the calixarene phenolic C_6 rings and the basal plane defined by the four phenolic oxygen atoms: 43.2(2)° for C(12) > C(17), 44.8(3)° for C(34) > C(39), 81.4(2)° for C(1) > C(6), and 87.0(3)° for C(23) > C(28).

Employment of the same reaction conditions and molar quantities as with **1** and **2**, but with the substitution of the neutral pillaring linker with 4,4′-azopy, gave **3** as red prisms. Again, the crystals were of suitable quality for single crystal X-ray diffraction but required synchrotron radiation to collect a data set of adequate quality for structural elucidation.[7] Analysis of this data reveals a similar extended 2-D bilayer sheet structure of formula $\{[Zn(OH_2)_2(L)(4,4'\text{-azopy})]\cdot DEF\}_n$, in which subtle differences in the coordination of the carboxylate groups compared to **1** gives rise to a different network topology. As with **1**, Zn_2L_2 dimers are formed by the monodentate binding of carboxylate groups from two calix[4]-arene molecules to single zinc atoms; however, intramolecular hydrogen bonding between one of the coordinated carboxylate oxygens and the ether oxygen of the same group with one of the phenolic OH groups forces the moiety to adopt a bent configuration. This has the effect of shortening one of the pendant carboxylate groups giving a dimeric unit in which calix[4]arene molecules are offset. The structure also differs from **1** in the coordination geometry observed around each metal center. Two 4,4′-azopy molecules coordinate to each metal center via their pyridinyl nitrogens; however, the

presence of two coordinated water molecules per zinc gives octahedral geometry (O(17) and O(18) at Zn(1) and O(19) and O(20) at Zn(2); Figure 7).
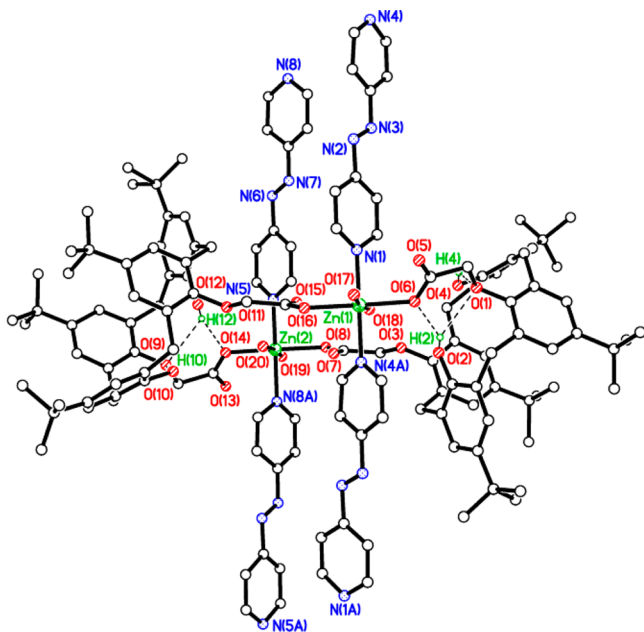

Figure 7. Diagram of the $Zn(OH_2)_2(L)(4,4'\text{-azopy})$ dimer in **3**, showing the coordination environment around the metal centers. Hydrogen atoms, except those involved in H-bonding interactions, are omitted. Hydrogen bonds are represented by dotted lines. Selected bond lengths (Å) and angles (°): Zn(1)−O(6) 2.094(5), Zn(1)−O(16) 2.074(4), Zn(1)−O(17) 2.147(5), Zn(1)−O(18) 2.116(6); N(1)−Zn(1)−O(16) 90.5(2), O(6)−Zn(1)−O(16) 172.7(2).

As in **1** and **2**, the calix[4]arene adopts a pinched conformation (and does not contain DEF molecules), in this example mediated by the presence of hydrogen bonding between the phenolic hydroxy groups and the acid functions, which precludes the presence of guest solvent molecules in the bowl of the calix[4]arene. Angles subtended by the calixarene phenolic C_6 rings and the basal plane defined by the four phenolic oxygen atoms: 35.3(2)° for C(12) > C(17), 35.9(3)° for C(34) > C(39), 75.53(19)° for C(1) > C(6), and 79.0(2)° for C(23) > C(28); 40.6(3)° for C(60) > C(65), 34.6(2)° for C(82) > C(87), 73.39(19)° for C(49) > C(54), and 79.19(19)° for C(71) > C(76). When viewed along the *a* axis, eight void spaces per unit cell are visible, located around the 4,4′-azopy molecules. Diffuse electron density observed in these void spaces was modeled using the PLATON squeeze procedure,[10] giving approximately half a DEF molecule per void space, or four per unit cell. The DEF molecules reside around the pyridyl linkers within the 2-D sheets, and these 2-D sheets lie in the *ab* plane. The calixarenes link pairs of Zn^{2+} ions together in the *b* direction via their carboxylate groups only, while the pyridyl ligands provide links parallel to *a* (Figures 8, 9, and S3).

Thermogravimetric Analysis. Thermogravimetric analyses were conducted on structures **1**, **2**, and **3** under an inert carrier flow of nitrogen to assess their porosities and solid state stabilities (Figure 10). Unexpectedly, for structure **1**, no weight loss was observed in the range 30−250 °C. This is in contradiction to the single crystal X-ray diffraction data, which offers evidence of 2.25 guest DEF molecules, and elemental

analyses which suggest the presence of two DEF molecules per formula unit. It can be concluded that either no guest solvent molecules were present in the sample analyzed, due to their removal during sample preparation, or that the solvent was encapsulated by the framework and was not removable until after the thermal decomposition had begun. Because of the similarities between this profile and those of structures **2** and **3** at temperatures above 280 °C, at which all three structures begin to thermally decompose, it is reasonable to assume that rather than being tightly bound within the framework, the guest DEF molecules were removed during sample preparation, which involved washing the sample with diethyl ether (see Experimental Section). The diethyl ether would have washed out the DEF molecules and then evaporated through the channels formed by the large and interconnected voids, especially those parallel to the crystallographic *b* axis.

Compounds **2** and **3** exhibit very similar TGA profiles, undergoing a weight loss of 9.7 and 11.1%, respectively, over the range 30−250 °C. In the case of **2**, this weight loss is attributable to the loss of two DEF molecules per formula unit (calculated 10.0%). The single crystal X-ray diffraction data suggest the presence of between one and two of these guest molecules (89 electrons recovered in total by the Platon Squeeze[10] procedure, but the larger void only accommodating 68 of these electrons and a DEF containing 56 electrons). The disorder/flexibility observed in the pyridinyl linker likely allows for a greater quantity of guest molecules to be accommodated, with elemental analyses conducted on **2** offering further evidence of the presence of a second DEF molecule per formula unit. For structure **3**, the loss of one DEF molecule and the two coordinated water molecules per formula unit equates to a loss of 11.9 wt %, which is in good agreement with the recorded TGA data. The presence of guest molecules is also supported by microanalysis, with the phase purity of the samples confirmed by the similarity in d-spacings for the collected and simulated powder X-ray diffraction patterns; note that the measured powder diffraction patterns include solvents in the voids, while the simulated patterns were calculated from CIF files that are solvent free, hence the slight differences, especially at low angle where disordered solvent makes a larger contribution (Supporting Information, Figures S4−S6). Thermal decomposition for all three structures commences at ∼280−300 °C as indicated by rapid and continuous weight loss. Since loss of all solvent of crystallization and water ligands is accounted for in **1**−**3**, what remains, prior to thermal decomposition, can be assumed to be the 2D metallocalixarene polymers. Because of the similarities in metal coordination modes between the structures, similar decomposition profiles are expected, with minor variations between the curves attributable to relative thermal stabilities of 4,4′-bipy, DPE, and 4,4′-azopy.

In summary, solvothermal syntheses involving the lower-rim functionalized diacid calix[4]arene 25,27-bis(methoxycarboxylic acid)-26,28-dihydroxy-4-*tert*-butylcalix[4]arene (**LH₂**), Zn-$(NO_3)_2\cdot6H_2O$, and the dipyridyl ligands 4,4′-bipyridyl (4,4′-bipy), 1,2-di(4-pyridyl)ethylene (DPE), or 4,4′-azopyridyl (4,4′-azopy) afforded a series of 2-D structures of the formulas ${[Zn(4,4'\text{-bipy})(L)]\cdot2^1/_4DEF}_n$ (**1**), ${[Zn_2(L)(DPE)]\cdot DEF}_n$ (**2**), and ${[Zn(OH_2)_2(L)(4,4'\text{-azopy})]\cdot DEF}_n$ (**3**) (DEF = diethylformamide). Crystal structure determinations (using synchrotron radiation for **1** and **3**) revealed for **1** the self-assembly of a 2-D extended bilayer structure of the formula ${[Zn(4,4'\text{-bipy})(L)]\cdot2^1/_4DEF}_n$ formed by the coordination of
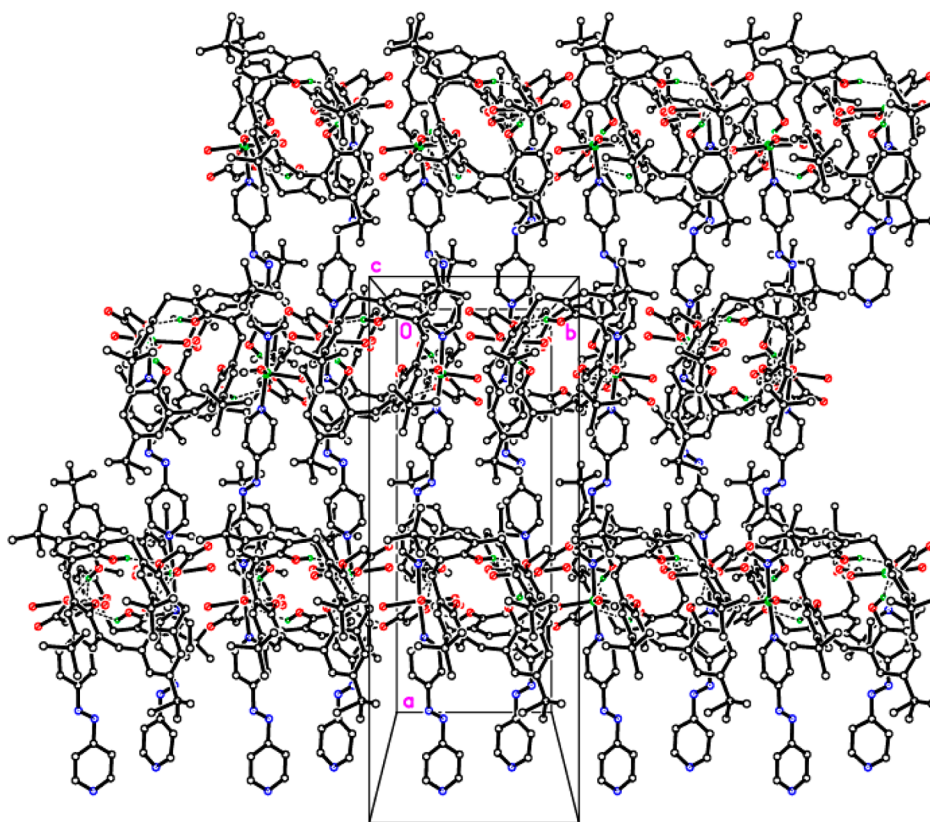
Figure 8. Diagram of **3** as viewed along the *c* axis, with linking 4,4′-azopy molecules forming the extended 2-D structure. Carbon atoms are represented by empty circles, with nitrogen, oxygen, and zinc atoms colored blue, red, and green, respectively. Hydrogen atoms, except those involved in H-bonding, which are represented by small green circles, are omitted.
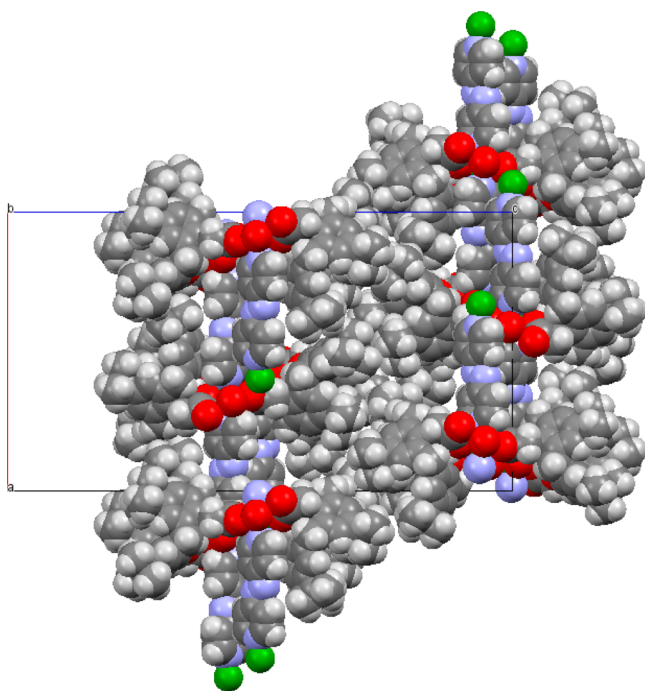

Figure 9. Packing plot of **3** using space filling atoms.

Figure 10. TGA data recorded for structures **1** (black), **2** (red), and **3** (blue).

4,4′-bipy molecules to Zn_2L_2 dimers, whereas the structure of **2** differs from that of **1** in both carboxylate coordination mode and packing. Specifically in **2**, four neighboring calix[4]arene units are linked via the coordination of one of the appended

acid moieties in a di-monodentate fashion to two zinc centers, giving a paddlewheel SBU. This coordination mode is observed at each of the acid moieties, giving infinite chains of the formula ZnL, observed along the *a* axis. In **3**, a similar extended 2-D bilayer sheet structure of formula $\{[Zn(OH_2)_2(L)(4,4′\text{-}azopy)]\cdot DEF\}_n$, in which subtle differences in the coordination of the carboxylate groups compared to **1** gives rise to a different network topology. As with **1**, Zn_2L_2 dimers are formed by the monodentate binding of carboxylate groups from two calix[4]arene molecules to single zinc atoms; however, intramolecular

Table 1. Crystallographic Data for Structures 1−3

structure	1	2	3
formula	$C_{58}H_{66}ZnN_2O_8\cdot2.25(C_5H_{11}NO)$	$C_{108}H_{126}Zn_2N_2O_{16}\cdot C_5H_{11}NO$	$C_{116}H_{140}Zn_2N_8O_{20}\cdot C_5H_{11}NO$
formula weight (g mol^{-1})	1212.08	1939.99	2198.24
crystal system	monoclinic	triclinic	orthorhombic
space group	$C2/c$	$P\bar{1}$	$Pna2_1$
unit cell dimensions			
a (Å)	17.8321(17)	10.539 (8)	26.249 (3)
b (Å)	46.606(4)	12.738 (10)	10.0932 (13)
c (Å)	18.9497 (18)	23.029 (19)	47.440 (6)
α (°)	90	103.240(16)	90
β (°)	114.056(6)	95.592(14)	90
γ (°)	90	91.319(17)	90
V (Å^3)	14381 (2)	2992 (4)	12569 (3)
Z	8	1	4
calculated density (Mg m^{-3})	1.120	1.077	1.162
adsorption coefficient (mm^{-1})	0.50	0.46	0.56
transmission factors (max, min)	0.995, 0.886	0.948, 0.725	0.989, 0.859
wavelength, λ (Å)	0.7749	0.71073	0.7749
crystal size (mm^3)	0.25 × 0.05 × 0.01	0.12 × 0.10 × 0.05	0.28 × 0.09 × 0.02
$2\theta_{max}$ (°)	24.3	27.3	33.1
reflections measured	44156	32328	104420
unique reflections	8869	12975	33131
R_{int}	0.075	0.070	0.053
reflections with $F^2 > 2\sigma(F^2)$	6524	10016	27271
number of parameters	736	747	1331
$R1$, $wR2$ $[F^2 > 2\sigma(F^2)]$	0.071, 0.213	0.125, 0.349	0.084, 0.224
GOF	1.03	1.06	1.02
largest difference peak and hole (e Å^{-3})	0.85 and −0.42	1.33 and −0.90	4.00 and −0.82

hydrogen bonding between one of the coordinated carboxylate oxygens and the ether oxygen of the same group with one of the phenolic OH groups forces the moiety to adopt a bent configuration. We have demonstrated the synthetic ability to deliberately incorporate in to a MOF, moieties with a potentially in-built void and known gas-uptake capability, although here the calix[4]arene adopts an empty, pinched-cone conformation.

■ EXPERIMENTAL SECTION

General. All reagents were purchased from Sigma-Aldrich and were used with no further purification. Solvents were purchased from Fisher Scientific. Tetrahydrofuran and ethanol were dried (where the use of dry solvents is specified) by heating to reflux over sodium and benzophenone and distilled and degassed prior to use. Infrared data (Nujol mulls, KBr windows) were collected using a Nicolet Avatar 360 FT IR spectrometer. Elemental analyses were performed by the National Elemental Analysis service at London Metropolitan University. Mass spectrometry data were recorded by the EPSRC National Mass Spectrometry Service Centre at Swansea University. TGAs were recorded on a TA Instruments 2950 TGA HR V5.3 thermogravimetric analyzer under an inert (N_2) carrier flow from 30 to 600 °C with a scanning rate of 2 °C min^{-1}.

Synthesis of {[Zn(L)(4,4′-bipy)]·2.25DEF}$_n$ (1). Ligand **LH$_2$** (0.5 mmol, 0.36 g), $Zn(NO_3)_2\cdot6H_2O$ (0.5 mmol, 0.15 g), and 4,4′-bipy (0.5 mmol, 0.08 g) were dissolved in a DEF/MeOH mixture (20 mL, 1:1). The solution was sealed in a 23 mL Teflon lined steel reaction vessel and heated to 75 °C for 96 h. The reaction vessel was then cooled at a rate of 2 °C h^{-1} to room temperature yielding 0.365 g colorless prisms (74% based on Zn). Elem. anal. calcd. for $C_{58}H_{66}N_2O_8Zn\cdot2C_5H_{11}NO$: C 68.81, H 7.47, N 4.72; found C 68.42, H 7.81, N 4.78%; IR/cm^{-1} (KBr): 3330(b), 2726(w), 2.667(w), 1651(s), 1615(s), 1592(s), 1535(w). 1481(s), 1418(w), 1363(s), 1305(s), 1276 (w), 1264(w), 1234(w), 1201(s), 1127(m), 1109(w),

1071(w), 1049(m), 965(w), 948(w), 917(w), 871(m), 816(m), 785(w), 764(w), 722(m), 700(w), 645(w).

Synthesis of {[Zn$_2$(L)$_2$(DPE)]·DEF}$_n$ (2). Ligand **LH$_2$** (0.5 mmol, 0.36 g), $Zn(NO_3)_2\cdot6H_2O$ (0.5 mmol, 0.15 g), and DPE (0.5 mmol, 0.09 g) were dissolved in a DEF/MeOH mixture (20 mL, 1:1). The solution was sealed in a 23 mL Teflon lined steel reaction vessel and heated to 75 °C for 96 h. The reaction vessel was then cooled at a rate of 2 °C h^{-1} to room temperature yielding 0.336 g pale yellow prisms (73% based on Zn) which were of suitable quality for single crystal X-ray diffraction. Elem. anal. calcd. for $C_{108}H_{126}N_2O_{16}Zn_2\cdot2C_5H_{11}NO$: C 69.43, H 7.31, N 2.74; found C 69.31, H 7.33. N 2.64; IR/cm^{-1} (KBr): 3412(s), 2725(w), 2667(w), 1662(s), 1612(s), 1559(w), 1545(w), 1507(w), 1365(s), 1343(w), 1328(w), 1303(w), 1290(w), 1264(w), 1245(w), 1194(m), 1164(w), 1123(w), 1108(w), 1097(w), 1072(w), 1039(m), 980(w), 931(w), 915(w), 871(m), 819(w), 800(w), 778(w), 761(w), 722(m).

Synthesis of [Zn(OH$_2$)$_2$(L)(4,4′-azopy)·DEF]$_n$ (3). Ligand **LH$_2$** (0.5 mmol, 0.36 g), $Zn(NO_3)_2\cdot6H_2O$ (0.5 mmol, 0.15 g), and 4,4′-azopy (0.5 mmol, 0.09 g) were dissolved in a DEF/MeOH mixture (20 mL, 1:1). The solution was sealed in a 23 mL Teflon lined steel reaction vessel and heated to 75 °C for 96 h. The reaction vessel was then cooled at a rate of 2 °C h^{-1} to room temperature yielding 0.328 g orange prisms (63% based on Zn). Elem. anal. calcd. for $C_{58}H_{70}N_4O_{10}Zn\cdot C_5H_{11}NO$: C 65.81; H 7.10; N 6.09; found C 65.54; H 7.11; N 6.05%; IR/cm^{-1} (KBr): 3417(s), 2725(w), 2661(w), 1648(m), 1632(s), 1594(w), 1580(m), 1484(s), 1363(s), 1339(w), 1301(m), 1266(w), 12.6(m), 1195(m), 1169(w), 1125(m), 1098(w), 1055(m), 1028(w), 976(w), 941(w), m 917(w), 871(m), 845(w), 835(w), 818(w), 803(w), 767(w), 723(m), 694(w), 668(w), 632(w).

Crystallography. Diffraction data for **1** and **3** were collected on a Bruker APEX 2 CCD diffractometer equipped with a silicon 111 monochromator on Station 11.3.1 at the ALS using synchrotron radiation.[11] Diffraction data for **2** were collected on a Rigaku Saturn 724+ CCD diffractometer using a rotating anode X-ray source and 10 cm confocal mirrors monochromator.[12] Data were corrected for absorption and Lp effects.[11,12] Structures were solved by direct

methods[13,14] and refined by full-matrix least-squares on F^2.[13,14] Further details are given in Table 1. H atoms were included in a constrained riding model. In **1** methyl groups within ᵗBu groups at C(18), C(31), and C(42) were modeled as disordered over two sets of positions with major components 57.1(12), 79.2(11), and 66.4(18)% respectively. Atoms C(54,55) and C(57,58) were also modeled as split over two sites with major component 72.6(16)%. The DEF solvent of crystallization was modeled as diffuse regions of electron density by the Platon Squeeze procedure which recovered 996 e⁻ per unit cell split between two voids, interpreted as nine DEF per void.[10] In **2** methyl groups within ᵗBu groups at C(8), C(18), C(29), and C(41) were modeled as disordered over two sets of positions with major components 80(4), 88.8(18), 56(4), and 92.0(10)% respectively. Atoms C(49) > C(54) were also modeled as split over two sites with major component 65.2(10)%. The DEF solvent of crystallization was modeled as a diffuse region of electron density by the Platon Squeeze procedure which recovered 89 e⁻ per unit cell of which 68 e⁻ was in one large void, interpreted as holding just one DEF.[10] The remaining electron density was distributed among six much smaller voids. In **3** the structure was modeled as a two-component inversion twin with a 51.9:48.1(13) component ratio. The DEF solvent of crystallization was modeled as a diffuse region of electron density by the Platon Squeeze procedure which recovered 32 or 36 e⁻ in each of eight small voids, interpreted as approximately half a DEF in each.[10] CCDC 964281−964283 contain the supplementary crystallographic data for this paper. These data can be obtained free of charge from The Cambridge Crystallographic Data Centre via www.ccdc.cam.ac.uk/data_request/cif.

■ ASSOCIATED CONTENT

Ⓢ Supporting Information

Diagrams of **1−3**; powder X-ray diffraction data for **1−3**; information about solvent voids for crystal structures **1−3** from the Platon Squeeze procedure; crystallographic information files. This material is available free of charge via the Internet at http://pubs.acs.org.

■ AUTHOR INFORMATION

Corresponding Author
*E-mail: c.redshaw@hull.ac.uk.
Notes
The authors declare no competing financial interest.

■ ACKNOWLEDGMENTS

■ REFERENCES

(1) See for example, (a) Liu, L.-L.; Li, H.-X.; Wan, L.-M.; Ren, Z.-G.; Wang, H.-F.; Lang, J.-P. *Chem. Commun.* **2011**, *47*, 11146. (b) Wan, L.-M.; Li, H.-X.; Zhao, W.; Ding, H.-Y.; Fang, Y.-Y.; Ni, P.-H.; Lang, J.-P. *J. Polym. Sci., Part A: Polym. Chem.* **2012**, *50*, 4864. (c) Casnati, A. *Chem. Commun.* **2013**, *49*, 6827.
(2) (a) Atwood, J. L.; Barbour, L. J.; Jerga, A.; Schottwel, B. L. *Science* **2002**, *298*, 1000. (b) Atwood, J. L.; Barbour, L. J.; Jerga, A. *Angew. Chem., Int. Ed.* **2004**, *43*, 2948. (c) Anachenko, G. S.; Moudrakovski, I. L.; Coleman, A. W.; Ripmeester, J. A. *Angew. Chem., Int. Ed.* **2008**, *47*, 5616. (d) Thallapally, P. K.; McGrail, P. B.; Dalgarno, S. J.; Schaef, H. T.; Tian, J.; Atwood, J. L. *Nat. Mater.* **2008**, *7*, 146.
(3) (a) Kajiwara, T.; Kobashi, T.; Shinigawa, R.; Ito, T.; Takaishi, S.; Yamashita, M.; Iki, N. *Eur. J. Inorg. Chem.* **2006**, 1765. (b) Bi, Y. F.; Wang, X. T.; Liao, W. P.; Wang, X. F.; Wang, X. W.; Zhang, H. J. *J. Am. Chem. Soc.* **2009**, *131*, 11650. (c) Liu, L.-L.; Ren, Z.-G.; Zhu, L. W.; Wang, H.-F.; Tan, W.-Y.; Lang, J.-P. *Cryst. Growth Des.* **2011**, *11*, 3479. (d) Liu, L.-L.; Ren, Z.-G.; Wan, L.-M.; Ding, H.-Y.; Lang, J.-P. *CrystEngComm* **2011**, *13*, 5718. (e) Kim, K.; Park, S.; Parl, K.-M.; Lee, S. S. *Cryst. Growth Des.* **2011**, *11*, 4059. (f) Liu, M.; Liao, W. P.; Hu, C. H.; Du, S. C.; Zhang, H. J. *Angew. Chem., Int. Ed.* **2012**, *51*, 1585. (g) Xiong, K. C.; Jiang, F. L.; Gai, Y. L.; Yuan, D. Q.; Han, D.; Ma, J.; Zhang, S. Q.; Hong, M. C. *Chem.—Eur. J.* **2012**, *18*, 5536. (h) Xiong, K. C.; Jiang, F. L.; Gai, Y. L.; Zhou, Y. F.; Yuan, D. Q.; Su, K. Z.; Wang, X. Y.; Hong, M. C. *Inorg. Chem.* **2012**, *51*, 3283. (i) Du, S. C.; Hu, C. H.; Xiao, J. C.; Tan, H. Q.; Liao, W. P. *Chem. Commun.* **2012**, *48*, 9177. (j) Xiong, K. C.; Jiang, F. L.; Gai, Y. L.; Yuan, D. Q.; Chen, L.; Wu, M. Y.; Su, K. Z.; Hong, M. C. *Chem. Sci.* **2012**, *3*, 2321. (k) Dai, F. R.; Wang, Z. Q. *J. Am. Chem. Soc.* **2012**, *134*, 8002. (l) Tan, H.; Du, S.; Bi, Y.; Liao, W. *Chem. Commun.* **2013**, *49*, 8211. (m) Zhang, Z.; Drapailo, A.; Matvieiev, Y.; Wojtas, L.; Zaworotko, M. J. *Chem. Commun.* **2013**, *49*, 8353.
(4) Liu, Y.-J.; Huang, J.-S.; Chui, S.S.-Y.; Li, C.-H.; Zuo, J.-L.; Zhu, N.; Che, C.-M. *Inorg. Chem.* **2008**, *47*, 11514.
(5) Redshaw, C.; Rowe, O.; Hughes, D. L.; Fuller, A. M.; Alvarado Ibarra, I.; Humphrey, S. M. *Dalton Trans.* **2013**, *42*, 1983.
(6) MacGillivray, L. R.; Atwood, J. L. *J. Am. Chem. Soc.* **1997**, *119*, 6931.
(7) Ma, B. Q.; Zhang, Y.; Coppens, P. *Cryst. Eng. Comm.* **2001**, *20*, 1.
(8) Nakamura, A.; Sato, T.; Kuroda, R. *Cryst. Eng. Comm.* **2003**, *56*, 318.
(9) (a) Clegg, W.; Elsegood, M. R. J.; Teat, S. J.; Redshaw, C.; Gibson, V. C. *J. Chem. Soc., Dalton Trans.* **1998**, 3037. (b) Clegg, W. *J. Chem. Soc., Dalton Trans.* **2000**, 3223.
(10) Spek, A. L. *Acta Crystallogr.* **1990**, *A46*, C34.
(11) *SAINT and APEX 2 Software for CCD Diffractometers*; Bruker AXS Inc.: Madison, WI, USA, 2009.
(12) *CrystalClear-SM Expert 2.0 r13*, Rigaku Corporation: The Woodlands, TX, 2011.
(13) Sheldrick, G. M. *Acta Crystallogr.* **2008**, *A64*, 112−122.
(14) Sheldrick, G.M., *SHELXTL User Manual*, version 6.12; Bruker AXS Inc.: Madison, WI, USA, 2001.